

## Dissecting the Akt/Mammalian Target of Rapamycin Signaling Network: Emerging Results from the Head and Neck Cancer Tissue Array Initiative

Alfredo A. Molinolo,<sup>1</sup> Stephen M. Hewitt,<sup>2</sup> Panomwat Amornphimoltham,<sup>1</sup> Somboon Keelawat,<sup>3</sup> Samraeung Rangdaeng,<sup>4</sup> Abelardo Meneses García,<sup>5</sup> Ana R. Raimondi,<sup>1</sup> Rafael Jufe,<sup>6</sup> María Itoiz,<sup>7</sup> Yan Gao,<sup>8</sup> Dhananjaya Saranath,<sup>9</sup> George S. Kaleebi,<sup>10</sup> George H. Yoo,<sup>11</sup> Lee Leak,<sup>12</sup> Ernest M. Myers,<sup>12</sup> Satoru Shintani,<sup>13</sup> David Wong,<sup>14</sup> H. Davis Massey,<sup>15</sup> W. Andrew Yeudall,<sup>15</sup> Fulvio Lonardo,<sup>11</sup> John Ensley,<sup>11</sup> and J. Silvio Gutkind<sup>1</sup>

**Abstract** **Purpose:** As an approach to evaluate the expression pattern and status of activation of signaling pathways in clinical specimens from head and neck squamous cell carcinoma (HNSCC) patients, we established the Head and Neck Cancer Tissue Array Initiative, an international consortium aimed at developing a high-density HNSCC tissue microarray, with a high representation of oral squamous cell carcinoma. **Experimental Design:** These tissue arrays were constructed by acquiring cylindrical biopsies from multiple individual tumor tissues and transferring them into tissue microarray blocks. From a total of 1,300 cases, 547 cores, including controls, were selected and used to build the array. **Results:** Emerging information by the use of phosphospecific antibodies detecting the activated state of signaling molecules indicates that the Akt-mammalian target of rapamycin (mTOR) pathway is frequently activated in HNSCC, but independently from the activation of epidermal growth factor receptor or the detection of mutant p53. Indeed, we identified a large group of tissue samples displaying active Akt and mTOR in the absence of epidermal growth factor receptor activation. Furthermore, we have also identified a small subgroup of patients in which the mTOR pathway is activated but not Akt, suggesting the existence of an Akt-independent signaling route stimulating mTOR. **Conclusions:** These findings provide important information about the nature of the dysregulated signaling networks in HNSCC and may also provide the rationale for the future development of novel mechanism-based therapies for HNSCC patients.

Carcinomas of the head and neck, including cancers originating from the oral cavity, oropharynx, hypopharynx, and larynx, represent the sixth most frequent type of cancer in the United States (1). The age-adjusted (world standard) incidence rate for total oral cavity and pharynx cancers were 8.3 per 100,000 population in 1994 to 1998, but varies greatly (range 4.8-17.7 per 100,000; ref. 2). More than 90% of head and neck cancers are squamous cell carcinoma (HNSCC). Although the use of

tobacco products and excessive alcohol consumption, as risk factors, are estimated to account for 75% of all oral cancers in the Western hemisphere (3, 4), the consumption of betel quid and derivatives constitutes the most important risk factor in Southeast Asia (4). Despite clear advances in our understanding of the biology of the disease and improvements in diagnosis and management of HNSCC, treatment options are limited, and patients with HNSCC frequently fail to respond to

**Authors' Affiliations:** <sup>1</sup>Oral and Pharyngeal Cancer Branch, National Institute of Dental and Craniofacial Research and <sup>2</sup>Tissue Array Research Program, Laboratory of Pathology, Center for Cancer Research, National Cancer Institute, NIH, Bethesda, Maryland; <sup>3</sup>Department of Pathology, Faculty of Medicine, Chulalongkorn University, Bangkok, Thailand; <sup>4</sup>Department of Pathology, Faculty of Medicine, Chiang Mai University, Chiang Mai, Thailand; <sup>5</sup>Patología, Instituto Nacional de Cancerología, Mexico DF, Mexico; <sup>6</sup>Laboratorio de Patología and <sup>7</sup>Department of Pathology, University of Buenos Aires School of Dentistry, Buenos Aires, Argentina; <sup>8</sup>Department of Oral Pathology, Peking University School of Stomatology, Beijing, China; <sup>9</sup>Reliance Life Sciences, Molecular Diagnostics and Genetics, Reliance Industries Ltd., Mumbai, India; <sup>10</sup>Medical University of Southern Africa (MEDUNSA), Limpopo, South Africa; <sup>11</sup>Department of Otolaryngology-Head & Neck Surgery and Oncology, Wayne State University, Detroit, Michigan; <sup>12</sup>College of Medicine, Howard University, Washington, District of Columbia; <sup>13</sup>Ehime University School of Medicine, Ehime, Japan; <sup>14</sup>School of

Dentistry, University of California at Los Angeles, California; and <sup>15</sup>Philips Institute of Oral and Craniofacial Molecular Biology, Virginia Commonwealth University, Richmond, Virginia

Received 5/1/07; revised 6/22/07; accepted 6/29/07.

**Grant support:** Intramural Research Program, National Institute of Dental and Craniofacial Research, NIH, and NIH RO1 grant RO1-DE15970 (D. Wong).

The costs of publication of this article were defrayed in part by the payment of page charges. This article must therefore be hereby marked *advertisement* in accordance with 18 U.S.C. Section 1734 solely to indicate this fact.

**Requests for reprints:** J. Silvio Gutkind, Oral and Pharyngeal Cancer Branch, National Institute of Dental and Craniofacial Research, NIH, 30 Convent Drive, Building 30, Room 212, Bethesda, MD 20892-4330. Phone: 301-496-6259; E-mail: sg39v@nih.gov.

©2007 American Association for Cancer Research.  
doi:10.1158/1078-0432.CCR-07-1041

standard therapies. Indeed, the 5-year survival rate of patients with advanced HNSCC (<50%) has improved only marginally over the past three decades (5). In this regard, ongoing efforts aimed at elucidating how the dysregulated activity of signaling molecules contributes to HNSCC progression may help identify new prognostic markers for the early diagnosis of premalignant lesions, as well as novel mechanism-based therapeutic approaches for the treatment of HNSCC patients.

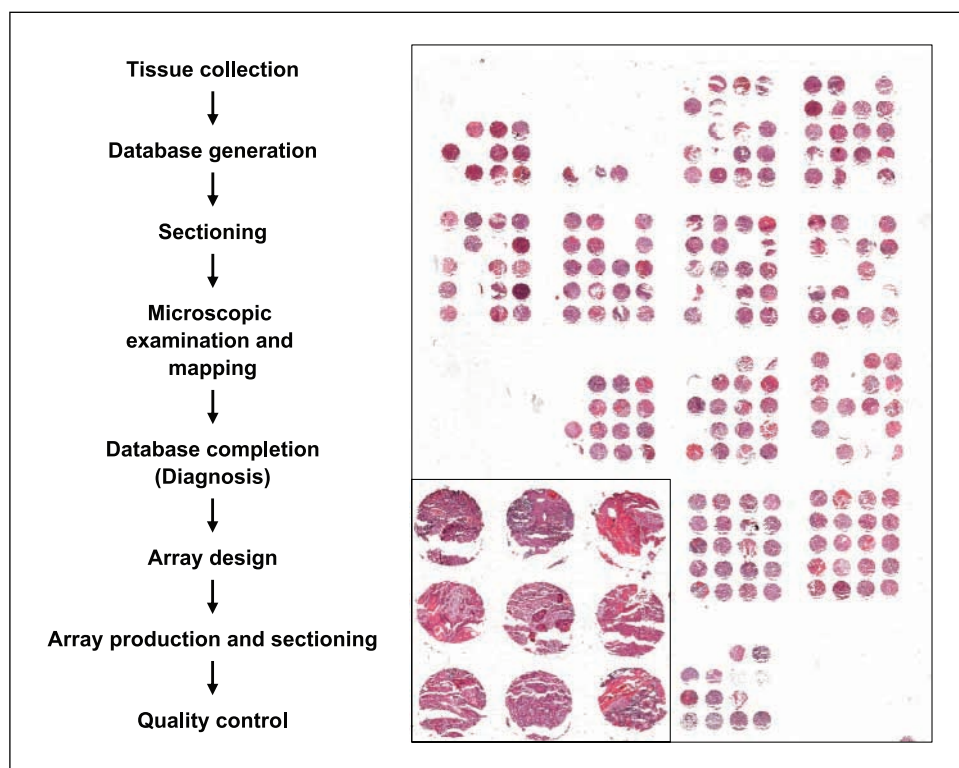
HNSCC often exhibit increased expression and activity of epidermal growth factor receptors (EGFR); mutations in *p53*; inactivation of the p16 tumor suppressor protein; overexpression of cyclooxygenase-2 (COX-2), cyclin D, *c-Myc*, and *Bcl<sub>XL</sub>*; and overactivity of the signal transducers and activator of transcription and nuclear factor- $\kappa$ B transcription factors (6–10). Recent work from our laboratory and others has also revealed that the persistent activation of the Akt signaling route is a frequent event in human HNSCC and their derived cell lines, and that activation of Akt is an early event in the carcinogenesis process, as judged by detailed studies in experimental animal models of squamous cell carcinoma (11–16). Furthermore, the accumulation of the phosphorylated active forms of Akt has been associated with progression from dysplasia to invasive carcinoma, and in turn the persistent activation of Akt contributes to the maintenance of the transformed phenotype as blockade of PDK1, a kinase acting upstream of Akt, induces tumor growth inhibition and cancer cell death (11).

Among the many molecules whose activity is regulated upon phosphorylation by Akt, the mammalian target of rapamycin (mTOR) pathway has recently received considerable attention, as its pharmacologic inhibition has already produced promising preclinical and clinical results in the treatment of many human malignancies exhibiting activation of the Akt-mTOR pathway (17). mTOR is an atypical serine/threonine kinase that

phosphorylates key eukaryotic translation regulators, including p70-S6 kinase (p70S6K) that phosphorylates the ribosomal protein S6, and the eukaryotic translation initiation factor 4E binding protein 1 (4E-BP1), which represses the eukaryotic translation initiation factor 4E (eIF4E; 18). In particular for HNSCC, *eIF4E* gene amplification and protein overexpression is often associated with malignant progression of HNSCC (19), and its expression levels in surgical margins can predict tumor recurrence (20). Furthermore, we have detected high levels of phosphorylated S6 (pS6), the most downstream target of the Akt-mTOR pathway, in a high fraction of HNSCC clinical samples and cell lines (21), and observed that inhibition of mTOR by the use of rapamycin causes the rapid decrease in the level of pS6 and the apoptotic death of HNSCC xenografts. However, the relationship between the status of activation of the Akt-mTOR pathway and other genetic and epigenetic molecular events contributing to HNSCC progression is still unknown.

On the other hand, with the recent progress in gene discovery and gene expression evaluation, and the development of thousands of new antibodies against potential tumor markers and signaling molecules, it has become clear that the real limiting step to make a contribution of clinical relevance to HNSCC patient is to have access to large collections of normal and tumor tissues in which the expression and activity status of relevant molecules can be explored simultaneously. For example, hundreds or even thousands of clinical specimens are required to ascertain the significance of a new diagnostic test or therapeutic target. This is often tedious with conventional molecular pathology technologies, and availability of such tissue resources is often rate limiting. To overcome this limitation, emerging technologies have now enabled the high-throughput molecular profiling of tissue specimens and target

**Fig. 1.** Successive steps in the array design and construction. The attached figure shows an H&E of one of the arrays to display the quality of the cores.



validation. Among them, one of the most widely used are the tissue microarrays (TMA), which are constructed by acquiring cylindrical biopsies from many (often 100-500) individual tumor tissues into a TMA block, which is then sliced to produce hundreds of sections for probing DNA, RNA, or protein targets (22). For example, a single immunostaining or *in situ* hybridization reaction can provide information on all of the specimens on the slide, whereas subsequent sections can be analyzed with other probes or antibodies. Here, we report the development of a HNSCC-specific TMA as part of a joint effort of the Head and Neck Tissue Array Initiative, a consortium of investigators from eight countries (Argentina, China, Japan, India, Mexico, South Africa, Thailand, and United States). A detailed description of this TMA is available to the scientific community upon request.<sup>16</sup> Furthermore, by the use of phosphospecific antibodies detecting the activated state of signaling molecules, we now show that the activation of the Akt-mTOR pathway is widespread in HNSCC, but independent from the activation state of EGFR or the detection of mutant p53. This approach also revealed the existence of a subgroup of patients in which the mTOR pathway is activated but not Akt, suggesting the existence of an Akt-independent signaling route stimulating mTOR in HNSCC. These findings contribute to the elucidation of the deregulated mechanism in HNSCC and may provide valuable information about suitable targets for the development of novel therapies for HNSCC patients.

## Materials and Methods

**Tissue microarray.** A total of 1,300 paraffin-embedded tissue blocks were contributed by the participating members of the Head and Neck Tissue Array Initiative, under an approved Research Activity Involving Human Subjects protocol, from the Office of Human Subjects Research, NIH, involving the use of anonymous normal and HNSCC tissues. Before analysis, H&E-stained section from each sample was evaluated and the suitability of inclusion for the study was determined. Five-micrometer sections were used for all subsequent analysis. A schematic diagram of the successive steps is depicted in Fig. 1. The tissue blocks were re-embedded if needed and an H&E section was obtained from each tissue for the re-evaluation of tissue preservation and diagnosis. The suitability of the tissue was evaluated using a number of inclusion criteria such as the size (1-2 mm in depth and at least 5 × 5 mm in length and width), as well as other features such as appropriate fixation, absence of significant electro-surgical device lesions, signs of acidic decalcifying agents, and the presence of usable tissue in each block. Data on initial diagnosis, site, staging, age, sex, and recurrence and survival were collected. Under these inclusion criteria, a total of 472 blocks were selected, including control squamous cell carcinomas from lung, skin, uterine cervix, and other tissues, as well as nonneoplastic squamous cell epithelium. The specific site data was missing in 93 cases that were identified only as HNSCC. Each H&E-stained slide was re-evaluated and mapped to identify the specific areas for tissue acquisition to build the TMAs, which were constructed using the approach described by Kononen et al. (23), using a Beecher manual tissue arrayer (MTA-1). Core diameter was 0.6 mm, and the sections were cut and covered with tape (Instrumedics; ref. 22).

**Immunohistochemistry.** All antibodies used were from Cell Signaling Technology, Inc., except for COX-2 and EGFR, and were diluted in 2.5% bovine serum albumin in PBS, as follows: p53, rabbit monoclonal antibody, 1:40; phosphorylated Akt (Ser<sup>473</sup>) rabbit monoclonal

antibody, 1:50; phosphorylated Akt (Thr<sup>308</sup>) rabbit monoclonal antibody, 1:25; phosphorylated EGFR (Tyr<sup>1068</sup>; 1H12) mouse monoclonal antibody, 1:100; and pS6 rabbit antibody, 1:100; COX-2, mouse monoclonal antibody, BD Transduction Laboratories, 1:100; EGFR, DAKO EGFR pharmDx kit for Manual Use, 1:10. The tissues slides were immersed in Safeclear II for dewaxing and detaching of the protective plastic layer for 30 min, three changes, hydrated through graded alcohols and distilled water, and washed with PBS. Antigen retrieval was done using a commercial unmasking solution (Vector Laboratories) or 10 mmol/L citric acid in a microwave for 20 min (2 min at 100% power and 18 min at 10% power). Slides were allowed to cool down for 30 min at room temperature, rinsed twice with PBS, and incubated in 3% hydrogen peroxide in PBS for 30 min to quench the endogenous peroxidase. The sections were then washed in distilled water and PBS and incubated in blocking solution (2.5% bovine serum albumin in PBS) for 1 h at room temperature. Excess solution was discarded, and the sections were incubated with the primary antibody diluted in blocking solution at 4°C overnight. After washing with PBS, the slides were sequentially incubated with the biotinylated secondary antibody (1:400; Vector Laboratories) for 30 min, followed by the avidin-biotin complex method (Vector Stain Elite, ABC kit; Vector Laboratories) for 30 min at room temperature. The slides were washed and developed in 3,3'-diaminobenzidine (Sigma FASTDAB tablet; Sigma Chemical) under microscopic control. The reaction was stopped in tap water, and the tissues were counterstained with Mayer's hematoxylin, dehydrated, and mounted. The number of positive cells was visually evaluated for each core and the results were expressed as a percentage of stained cells/total number of cells (24). According to their immunoreactivity, the tissues array cores were divided into five categories: 0, less than 10% of stained cells; 1, between 10% and 25%; 2, between 25% and 50%; 3, 50% to 75%; and 4, 75% to 100% of cells stained. For further cluster analysis, the data obtained, recorded in Microsoft Excel format, was converted into scaled values centered on zero (e.g., a score of 0 is converted to -2, 2 to 1, and 4 to 3). These converted data, in simple text file, was then used for further statistical analysis and hierarchical clustering. The hierarchical analysis was done using Cluster program with average linkage based on Pearson's correlation coefficient as the selection variable.<sup>17</sup> The results were visualized using the TreeView program. The clustered data were arranged with markers on the horizontal axis and tissue samples on the vertical axis. Two biomarkers with a close relationship are located next to each other. Cases with 50% or less interpretable scores or missing cores were excluded from this analysis.

**Statistics.** Covariation of the expression of the different markers was analyzed with the nonparametric Spearman correlation (Spearman's rank correlation test) with two-tailed *P* values, and 99% confidence, using GraphPad Prism 4.03 (GraphPad Software). Differences in immunohistochemical reactivity between normal tissues and HNSCC classified into differentiation groups were analyzed using the Kruskal-Wallis test for non-Gaussian populations (nonparametric ANOVA) followed by the Dunn's posttest to compare all pairs of columns (GraphPad Software).

## Results

**Array construction and design.** Tissues contributed by members of the Head and Neck Tissue Array Initiative (~1,300 paraffin-embedded tissue blocks) were processed as outlined in Fig. 1. The most common cause of exclusion was reduced size, but many tissues were also excluded because of their poor fixation, damage by the use of electro-surgical devices, and cell acidophilia compatible with the use of acidic decalcifiers, which are associated with low recovery of antigenic

<sup>16</sup> <http://www.nidcr.nih.gov/Research/ResearchResources/HeadandNeckTissueArrayInitiative.htm>

<sup>17</sup> <http://rana.lbl.gov/EisenSoftware.htm>

protein. A total of 472 HNSCC cases with varying degrees of differentiation were selected. Seventy-five additional controls, including 37 cores corresponding to normal tissues (liver, lymph node, bone marrow, muscle, thyroid, pancreas, spleen, breast, cerebellum, cerebrum, endometrium, placenta, kidney, skin, lung, salivary glands, and colon), were obtained from the Tissue Array Research Program, National Cancer Institute, and included in each array. Two different array blocks were engineered, one including tissues from South and North America and South Africa (253 cores, including controls), and the other from all Asian countries (254 cores including normal tissue controls). The distribution of HNSCC selected cases per country is represented in Fig. 2A. Specific sites of tissue origin for the HNSCC as well as control (squamous cell carcinoma from esophagus, uterine cervix, vulva, penis, and skin) are shown in Fig. 2B.

**Distribution of cases.** From the cases of known origin, the vast majority, 322 cases, corresponded to squamous cell carcinoma that originated in the oral mucosa, 156 to extraoral

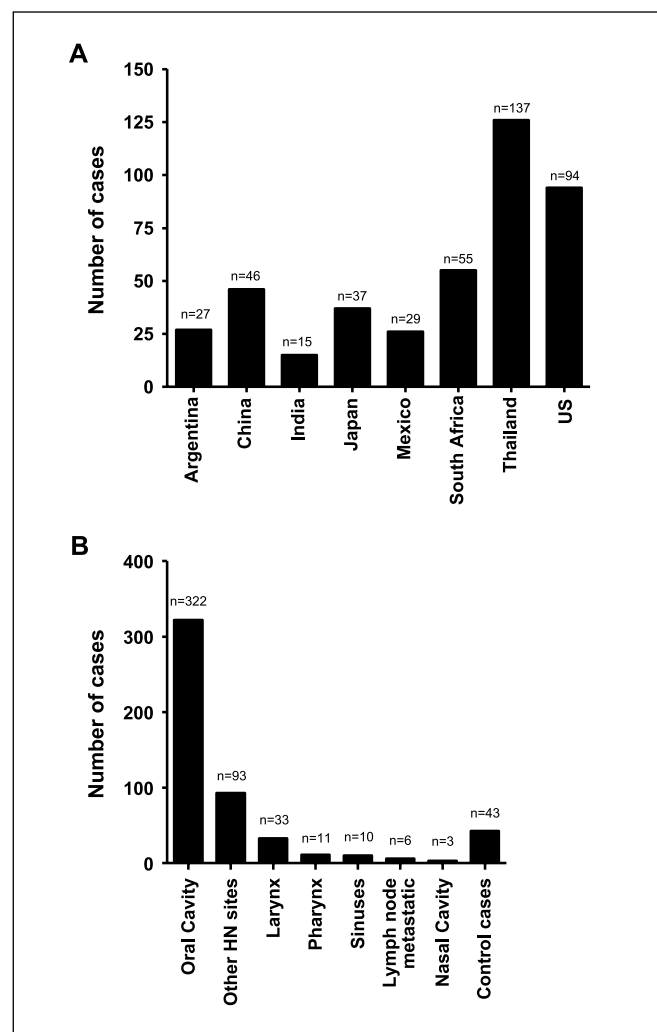


**Fig. 2.** A, distribution of the array cases according to country of origin, representing exclusively the cases selected for the array, rather than the total number of cases submitted. B, distribution of the array cases according to site of origin of the tumors. Most of the tumors selected were originated in the mucosa of the mouth; the array also includes a series of control cases, such as uterine cervix and skin carcinomas.

HNSCC from different sites, and 43 cases of normal tissues and control squamous cell carcinoma from sites other than the head and neck (Fig. 2B). The distribution of cases based on their differentiation was similar across countries, without any significant differences; ~40% of the cases were well-differentiated carcinomas, 37% were moderately differentiated, and 23% were poorly differentiated. However, most tumors are morphologically heterogeneous, and therefore it is difficult to map precise areas of the tissue block from where the punching needle could procure homogeneous tissues. Thus, some squamous cell carcinomas may show areas with more than one degree of differentiation, even with a needle of 0.6 mm in diameter. On the other hand, we noticed also that sections taken at different depths of a given tumor sometimes show slightly different characteristics or, as it happens in few cases; no tumor tissue at all in some cores, and particularly in the last sections of each block. Nonetheless, the quality of the different cores was in general good, and we considered each tissue array section acceptable if >70% of the cores had tumor samples. Furthermore, some of the expected limitations of the tissue arrays (23) were partially overcome by sampling from more than one tumor region per paraffin block to build numerous array blocks from the same group of samples.

**Immunohistochemistry.** As part of a joint effort aimed at investigating the nature of the deregulated molecular mechanism, including aberrant activity of signaling pathways, we next explored the expression level and/or status of activation of a number of signaling molecules in these HNSCC tissue arrays. In this regard, although the potential loss of some phosphoproteins can occur during the paraffinization process, currently available technique and the widespread use of phosphospecific antibodies suggest that paraffin-embedded tissues retain most of their phosphorylated protein species. In particular for this study, we focused on molecules involved in the EGFR-Akt-mTOR signaling pathway, and two proteins whose expression is often associated with HNSCC progression, p53 and COX-2. All selected antibodies used were first tested in relevant samples of HNSCC and in nonneoplastic squamous epithelia to confirm their applicability to paraffin-embedded tissues as well as to set up optimal conditions, such as appropriate antibody concentrations and antigen unmasking approaches. In addition, sections from nonneoplastic oral mucosa and additional normal tissues were used to establish the specificity and baseline detection for all the proteins studied.

Examples of immunohistochemical results of selected array cases are shown in Fig. 3. Figure 3 shows the H&E staining of a representative moderately differentiated HNSCC of one of the array samples. Immunodetection of p53 in this particular case (Fig. 3) revealed intense nuclear staining in a large proportion of tumor cells. EGFR and phosphorylated EGFR (pEGFR) showed mostly membrane staining, with pEGFR occasionally exhibiting a punctuate pattern. EGFR immunoreactive cells were uniformly distributed throughout the carcinomas; however, pEGFR stained a higher number of cells in the more differentiated areas. Both Akt phosphorylated forms, pAkt<sup>Ser473</sup> and pAkt<sup>Thr308</sup>, were stained in the cytoplasm, with pAkt<sup>Ser473</sup> also showing some nuclear staining. The immunodetection of pS6 disclosed a strong cytoplasmic staining in most tumor cells; a high proportion of neoplastic cells also displayed a strong cytoplasmic immunoreactivity for COX-2. The proportion of

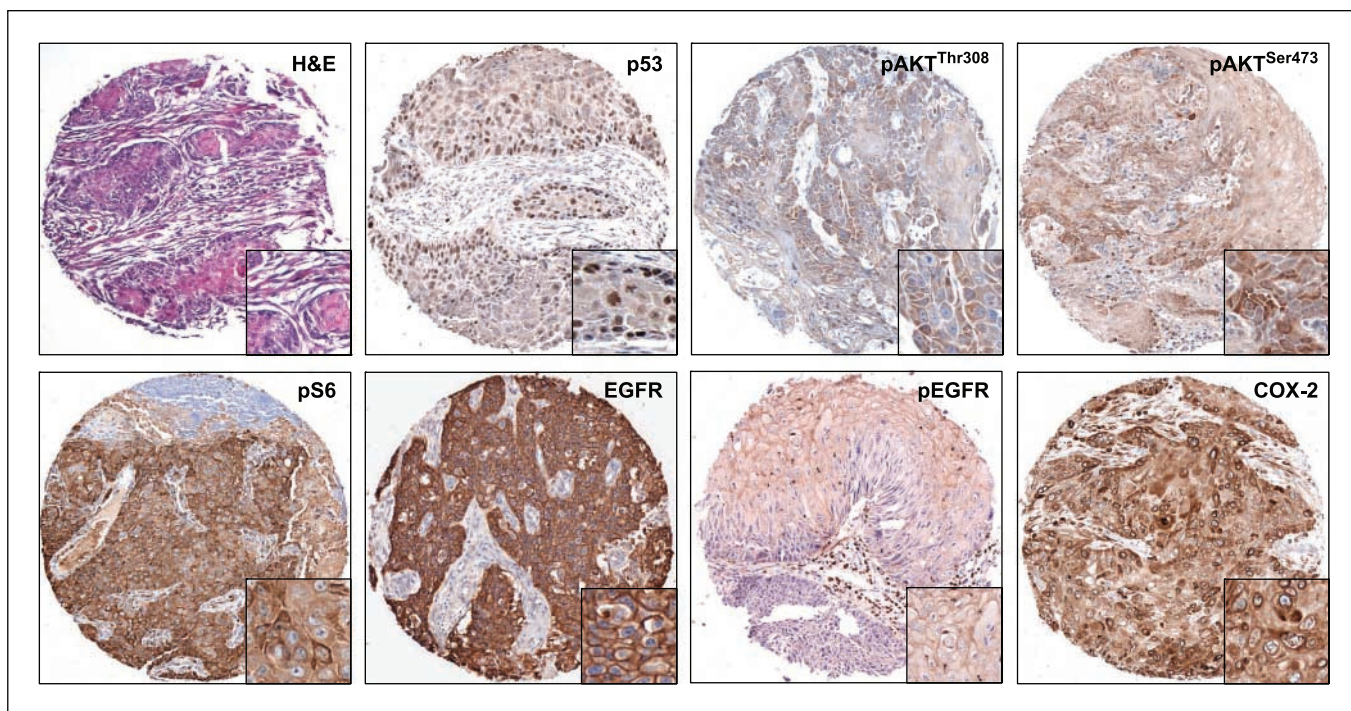


**Fig. 3.** Representative H&E sample and immunohistochemistry studies of the protein markers in different array cores. The H&E picture shows a core corresponding to a moderately differentiated squamous cell carcinoma with good tissue preservation; this tissue quality is representative of most of the array cores. p53 immunoreactivity was restricted to the nuclei of malignant cells. Both phosphorylated forms of Akt gave cytoplasmic positive reaction, with pAkt<sup>Thr308</sup> occasionally showing nuclear immunostaining. pS6 was strongly positive exclusively in the cytoplasm. EGFR showed strong membrane staining, with occasionally cytoplasmic reactivity. The distribution was even throughout the structure of the tumors, with no obvious differentiation-related pattern. pEGFR also disclosed membrane staining, which was strongest along the more differentiated areas of the tumors. COX-2 was positive within the cytoplasm of malignant cells with an even distribution. Magnification,  $\times 40$ ; insets,  $\times 100$ .

pS6 immunoreactive cells was higher in areas closer to the invasive, border of the tumors.

In general, three TMA slides were used for each immunostaining, scoring the percentage of stained cells as well as the number of cases immunoreactive for each protein. Figure 4 shows a detailed analysis of the array cores according to the concurrent staining of the different proteins in the same cores. For example, from a total of 305 cores evaluated for immunostaining of p53, 182 (60%) gave positive nuclear staining. More than 90% of the samples were positive for both pAkt<sup>Ser473</sup> and pS6, aligned with their functional relationship with mTOR. The fraction of overall cases positive for pAkt<sup>Thr308</sup> was overall slightly less than those positive for pAkt<sup>Ser473</sup> (95% versus 99%). Remarkably, however, the number of cells staining positive for pAkt<sup>Ser473</sup> in each case was higher than those displaying positive staining for pAkt<sup>Thr308</sup> (Fig. 4). Intense staining for EGFR was detected in 97% of all cases, whereas staining for pEGFR<sup>Tyr1068</sup>, which detect its active form, was positive in  $\sim 47\%$  of the cases. Overexpression of COX-2 was also identified in most of the tumors examined, giving positive cytoplasmic immunoreactivity in 96% of the cases.

**The Akt-mTOR signaling network in HNSCC.** When the percentage of stained cells scored in the HNSCC cases was evaluated against normal tissues, as shown in Fig. 5, all markers were significantly higher in HNSCC across all degrees of differentiation, except for pEGFR. Interestingly, the Kruskal-Wallis test also showed significant differences in favor of the more differentiated tumors for some molecules, such as

between well and poorly differentiated tumors for pS6 staining ( $P < 0.001$ ), and between well and poorly differentiated ( $P < 0.0001$ ) and moderately and poorly differentiated tumors for COX-2.

The Spearman rank test showed significant correlation between the proteins of the Akt-mTOR pathway, pAkt<sup>Thr308</sup>, pAkt<sup>Ser473</sup>, and pS6 (Table 1), and these results were nicely

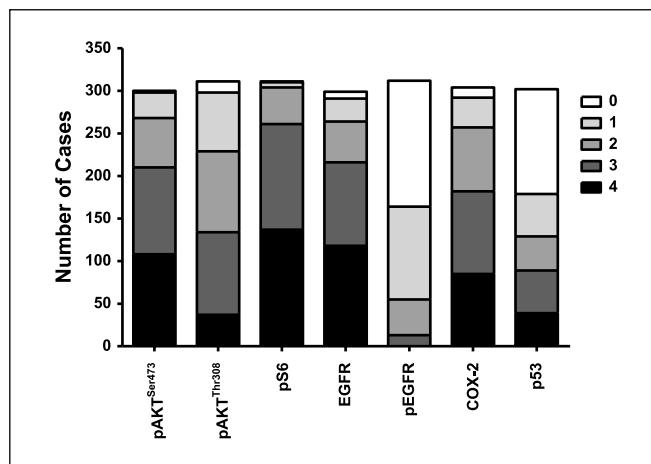


**Fig. 4.** Immunohistochemical reactivity of seven protein markers in representative cases of the HNSCC. The graphics shows a significant activation of the Akt-mTOR (Akt<sup>Ser473</sup>, pAkt<sup>Thr308</sup>, and pS6) pathway, and suggests a lack of direct correlation with one of its upstream activators, EGFR. Approximately 60% of the array cases were positive for p53, and  $>90\%$  immunoreacted with the COX-2 antibody.

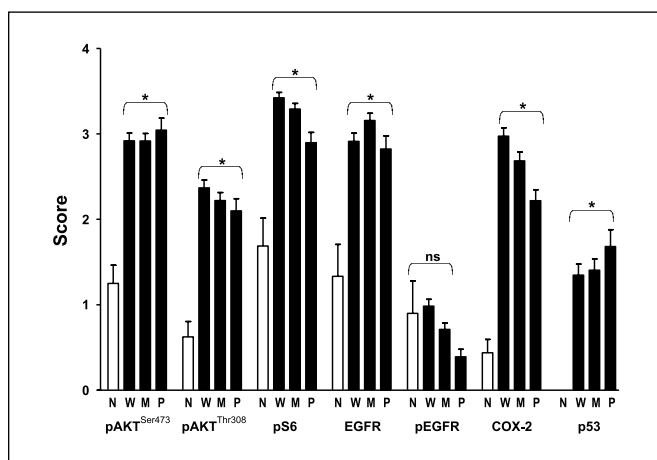


**Fig. 5.** Distribution of immunoreactivity segregated by differentiation groups. Differences in normal (N) versus well differentiated (W), moderately differentiated (M), and poorly differentiated (P) groups were significant (\*) for all proteins except pEGFR (NS). In the pS6 group, significant differences were found between well versus poorly differentiated ( $P < 0.001$ ); in pEGFR, between well versus poorly differentiated ( $P < 0.001$ ) and moderately versus poorly differentiated ( $P < 0.01$ ); in COX-2, between well versus poorly differentiated ( $P < 0.001$ ) and moderately versus poorly differentiated ( $P < 0.01$ ).

reflected by the cluster analysis (Fig. 6). No significant correlation between p53 and EGFR or pEGFR was observed. Interestingly, we observed that 46% of the cases positive for pAkt<sup>Ser473</sup> and 43% of the cases positive for pAkt<sup>Thr308</sup> were negative for pEGFR. COX-2, which was expressed in a high proportion of cases, correlated well with the activation of the mTOR pathway, but less strongly with pAkt<sup>Ser473</sup> compared with pAkt<sup>Thr308</sup> and pS6. p53 behaved as an independent marker and did not show any correlation with the other proteins investigated.

The availability of hundreds of tumor tissues, in which the majority or all selected markers were analyzed simultaneously, enabled us to use bioinformatic tools to generate unsupervised, hierarchical clusters on the basis of their similarities over the expression of seven biomarkers (Fig. 6). A total of 2,289 data points were included in this analysis of immunostaining results from tissue cores. The cluster analysis was done only in samples for which staining of at least four of the seven markers were available (327 HNSCC samples and 9 normal oral tissues). A heatmap approach was used to represent the percentage of

stained cells according to the scoring systems used for Fig. 4, as described in Materials and Methods. Tissues scored as 0 were represented as green; 1, as black; 2, as dark red; and 3 as red. No available data was represented as gray. In the heatmap shown in Fig. 6, the length and the subdivision of the branches displays the relatedness of the HNSCC (left) and the protein expressions (top). As expected, pS6 and pAkt<sup>Ser473</sup> and pAkt<sup>Thr308</sup>, and even EGFR clustered together; however, pEGFR and p53 were distantly related to these molecular markers. Interestingly, using this unsupervised clustering approach, the HNSCCs were clearly separated from normal tissues, reflecting the robustness of the algorithm (Fig. 6). Of note, a clear separation of certain clusters was also revealed by this analysis. For example, in a group depicted as cluster 1, all samples were negative for pEGFR but were positive for p53, and show activation of Akt and phosphorylation of pS6. In a subgroup of HNSCCs (cluster 2), many of the tumors were negative for pEGFR and/or p53, but have high levels of pS6 and Akt phosphorylated in both of its activation sites and do not display immunoreactive COX-2. Surprisingly, there is at least one HNSCC subgroup that is different from the rest in that these HNSCCs display negative staining for pEGFR, p53, and pAkt<sup>Thr308</sup>, whereas they are weakly stained for pAkt<sup>Ser473</sup>, but still have high levels of expression of pS6 (cluster 3). Thus, emerging clustering analysis suggest that EGFR activation is not closely related with the activation of Akt and its downstream target, mTOR. Furthermore, this approach revealed the existence of multiple subpopulations of HNSCC patients, which are distinguishable based on p53 immunoreactivity and the activation status of EGFR and signaling molecules of the Akt-mTOR pathway.

## Discussion

In a constantly shrinking world with its often unpredictable migration patterns, it is clear that international collaborative efforts are necessary to identify key molecular events driving HNSCC progression across all previously perceived geographic, cultural, and socioeconomic boundaries. In response to these needs, we established the Head and Neck Tissue Array Initiative, a multinational collaborative effort aimed at building a TMA including representative oral cancer cases from around the world, to begin dissecting the complexity of the dysregulated signaling networks involved in HNSCC progression. We describe here the first-generation HNSCC TMA and provide

**Table 1.** Spearman rank test analyses of the array immunostainings

Protein	pAkt <sup>Thr308</sup>	pS6	EGFR	pEGFR	COX-2	p53
pAkt <sup>Ser473</sup>	$n = 288$ ( $P < 0.0001$ )	$n = 288$ ( $P < 0.002$ )	$n = 276$ ( $P < 0.005$ )	$n = 283$ (NS)	$n = 279$ ( $P < 0.05$ )	$n = 273$ (NS)
pAkt <sup>Thr308</sup>		$n = 301$ ( $P < 0.0001$ )	$n = 283$ (NS)	$n = 293$ (NS)	$n = 290$ ( $P < 0.005$ )	$n = 285$ (NS)
pS6			$n = 289$ (NS)	$n = 299$ (NS)	$n = 295$ ( $P < 0.0001$ )	$n = 288$ (NS)
EGFR				$n = 289$ (NS)	$n = 286$ ( $P < 0.0001$ )	$n = 282$ (NS)
pEGFR					$n = 297$ (NS)	$n = 291$ (NS)
COX-2						$n = 290$ (NS)

NOTE: The values represent number of common cores analyzed ( $n$ ) and  $P$  values. Strong correlation is seen between the proteins of the Akt-mTOR pathway, independently of the status of activation of EGFR. p53 behaves as an independent variable, showing no correlation with the other proteins analyzed.

Abbreviation: NS, not significant.

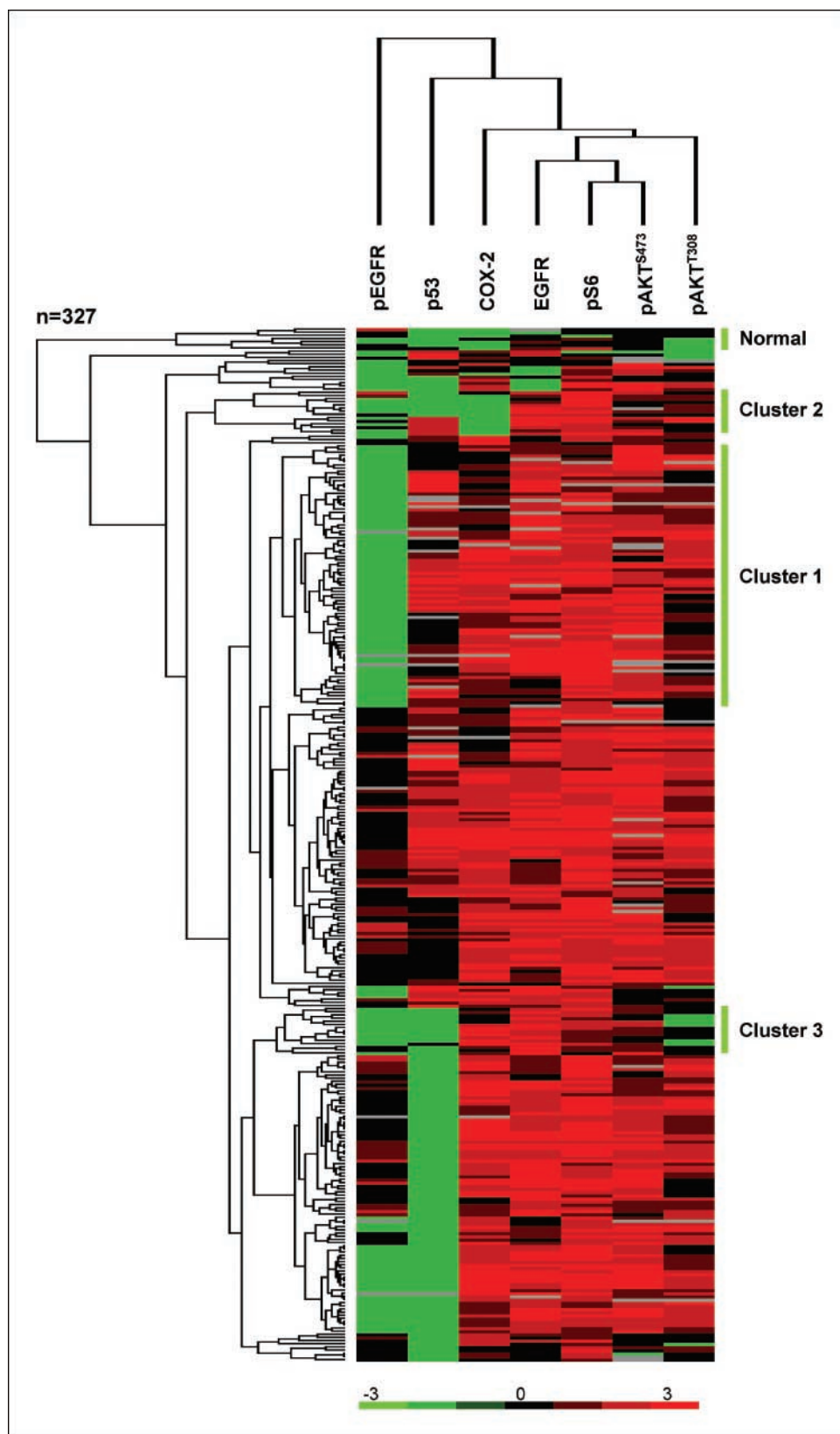


**Fig. 6.** Clustering analyses. The closeness of the columns directly indicates correlation. There is a strong correlation between pS6, pAkt<sup>Thr308</sup>, and pAkt<sup>Ser473</sup>; COX-2 also correlates strongly, whereas p53 and pEGFR segregate independently.

evidence that alterations of the Akt-mTOR pathway are shared by most HNSCC cases, independently of their country of origin, status of activation of EGFR, and the detection of mutant forms of *p53*.

The two isoforms of cyclooxygenase enzymes, COX-1 and COX-2, catalyze the rate-limiting step in the conversion of arachidonic acid into prostaglandins and thromboxanes (25). COX-1 is constitutively expressed in various tissues but COX-2

expression is usually undetectable in oral mucosa (26). However, clinical and experimental evidence suggests that COX-2 expression is an early event in carcinogenesis, and that the consequent release of prostaglandins, which act as potent inflammatory mediators, is a key event in tumor progression and metastasis (26–29). The expression of this enzyme has been shown in 70% to 88% of specimens from patients with HNSCC using immunohistochemistry (30) and in 87% of tumor specimens using reverse transcription-PCR (31). In line with these prior reports, COX-2 was detected by immunohistochemistry in ~90% of the array cases, which further supports the link between inflammation and carcinogenesis in HNSCC, and confirms the suitability of our tissue arrays to explore the expression pattern of molecules of biological significance in HNSCC progression.

The nuclear accumulation and subsequent detection by immunohistochemistry of the product of the *p53* gene, which has been described in 50% to 70% of human HNSCC, has been often used as indirect marker to examine the presence of inactivating mutations in *p53* (27, 32, 33). *p53* may also harbor mutations that do not result in its stabilization or, alternatively, *p53* function may be inhibited by epigenetic events, such as by enhancing its degradation or by interference with proteins controlling its transcriptional activity (34). In our study, we found that 60% of the cases were positive for *p53*, a result aligned with previous published reports (35). Of interest, although *p53* mutations are linked to tobacco carcinogens (36), we were not able to find a significant difference in the number of *p53*-positive cases when comparing tissue samples from Asian countries in which betel nut, rather than tobacco use, represents a risk factor and which, therefore, would have been predicted to exhibit a lower incidence of *p53* mutations (37, 38). The future development of HNSCC TMAs, including detailed clinical information, may be required to address this issue in detail. We also failed to observe a correlation between *p53* staining and EGFR levels or its activation status, further supporting that these are two independent events in HNSCC progression (39).

EGFR, a member of the ErbB family of growth factor receptor tyrosine kinases that is expressed in most cells of epithelial origin, plays multiple roles in HNSCC progression (40, 41). As expected, >90% of the tissue array tumors that were examined expressed high levels of EGFR (42). However, the status of activation of the EGFR pathway in HNSCC is reported to vary widely from 5% to 90% (27, 42). In fact, only 50% of the HNSCC tissues reacted with a phosphospecific antibody against the Tyr<sup>1068</sup> phosphorylated form of EGFR, pEGFR, which represents the active form of this receptor (43, 44). These findings are aligned with those recently reported by others in which the activity of EGFR was determined in a HNSCC tissue array using a FRET-based assay to determine the activation state of EGFR (42).

On the other hand, pharmacologic and biological approaches aimed at suppressing HNSCC cell growth and progression by inhibiting EGFR have not achieved the expected success (45–47). Thus, although EGFR plays an important role in the pathogenesis of HNSCC, emerging evidence supports the existence of EGFR-independent pathways that may promote the growth and survival of HNSCC tumor cells, thus rendering EGFR inhibitors ineffective as a single therapeutic agent (41). For example, persistent signal transducers and activators of

transcription 3 tyrosine phosphorylation, Akt activation, and mTOR-dependent phosphorylation of ribosomal S6 protein can occur even in HNSCC cells that do not display highly active EGFR signaling (11, 21, 48), supporting the existence of EGFR-independent pathways that may contribute to HNSCC progression.

Indeed, in line with previous work from our laboratory and others (11, 12, 15), Akt was activated in a high proportion of the tumors examined, as judged by the immunodetection of its Ser<sup>473</sup> and Thr<sup>308</sup> phosphorylated forms. Upon EGFR stimulation, Akt is activated in a multistep process that involves the stimulation of the activity of phosphatidylinositol 3'-OH kinase by EGFR-dependent phosphorylation and recruitment to the membrane of the phosphatidylinositol 3'-OH kinase p85 subunit. This leads to the accumulation of phosphatidylinositol 3,4,5-triphosphate, which binds the Akt pleckstrin homology domain, thereby causing the recruiting of Akt to the plasma membrane and the phosphorylation of Thr<sup>308</sup> on Akt by PDK1 (49). Akt activation then leads to the stimulation of the mTOR signaling pathway, and subsequently mTOR phosphorylates Akt at Ser<sup>473</sup> (50). Both phosphorylation events are required for full activation of the kinase activity of Akt (51). In turn, Akt plays a critical role in cell survival and normal cell growth, and is frequently activated in a wide variety of neoplastic diseases such as colorectal, ovarian, lung, and breast cancer (51, 52).

In a previous study using a mouse model of chemically induced squamous carcinoma, we observed that an increase in the kinase activity of Akt is an early preneoplastic event in squamous cell carcinogenesis (14). Furthermore, expression of Akt accelerates tumor progression and promotes the malignant conversion of immortalized murine keratinocyte cell lines (14, 16). In a recent study, we observed that Akt activation is a frequent event in human HNSCC and that active Akt detected in these tumors correlates with tumor progression (11). In fact, in line with a likely role of Akt in HNSCC development, the presence of its active form was recently found to be a marker of poor prognosis (15). In agreement with the findings that Akt acts downstream from EGFR (52), the majority of the tumors exhibiting elevated pEGFR staining were also positive for pAkt<sup>Thr308</sup> and pAkt<sup>Ser473</sup>. However, nearly half of the cases in which these phosphorylated species of Akt were detected occurred in tumor samples in which EGFR was not persistently activated. These findings provide further support to the existence of yet to be fully defined molecular alterations in HNSCC, which may lead to the EGFR-independent activation of Akt. In this regard, gene amplification and overexpression of the  $\alpha$  subunit of phosphatidylinositol 3'-OH kinase has been observed in a large fraction of HNSCC (53–55), and the presence of an activating mutation in this enzyme has been recently reported (56, 57). Similarly, decreased expression or activity of PTEN, a phosphatidylinositol 3,4,5-triphosphate phosphatase, either by the result of genetic or epigenetic events, has been recently reported in HNSCC (54, 58). Thus, the aberrant function of molecules controlling the synthesis and degradation of phosphatidylinositol 3,4,5-triphosphate, phosphatidylinositol 3'-OH kinase, and PTEN may help explain the presence of activated Akt in the absence of persistent EGFR signaling. This, as well as the possibility that other overactive tyrosine kinase growth factor receptors, such as c-Met or HER2 (59, 60), may result in the EGFR-independent stimulation of Akt in HNSCC, warrants further investigation.



Of interest, a surprising observation in this TMA analysis was that the proportion of HNSCC cases that were positive for Akt<sup>Thr308</sup> was smaller than that of Akt<sup>Ser473</sup>. The presence of this subgroup of cases positive for Akt<sup>Ser473</sup> but negative for Akt<sup>Thr308</sup> suggests that the simultaneous presence of both phosphorylated forms may not be strictly necessary for tumor progression. Of note, the most prominent kinase phosphorylating Akt on Ser<sup>473</sup> seems to be mTOR, which is itself a downstream target of the Akt signaling pathway (18). This raises the possibility of the existence of a group of HNSCC patients in which mTOR is activated by molecular alterations impinging downstream of Akt, thereby bypassing the need for a fully active Akt for tumor progression. This possibility is supported by the presence of pS6, one of the most downstream target molecules of mTOR, in the majority (92%) of the cases in which Akt is phosphorylated in Ser<sup>473</sup>, likely by mTOR, irrespective of the status of Akt activation by phosphorylation at Thr<sup>308</sup>.

But how can be mTOR become activated in pAkt<sup>Thr308</sup>-negative tumors? Recent findings may provide a clue. In particular, the ability of Akt to coordinate growth-promoting signaling with nutrient-sensing pathways controlling protein synthesis through mTOR may represent an essential mechanism whereby Akt ultimately regulates cell proliferation (61). The pathway by which Akt controls mTOR is initiated by Akt phosphorylation and inactivation of a tumor-suppressor protein, tuberous sclerosis complex protein 2 (TSC2), which is also known as tuberin (62). TSC2 associates with a second tumor-suppressor protein, tuberous sclerosis complex protein 1 (TSC1), and these act together as a GTPase-activating protein for the small GTPase Rheb1 (62). Thus, inactivation of TSC2 by Akt leads to the accumulation of the GTP-bound (active) form of Rheb1, which, in turn, promotes the phosphorylation and activation of mTOR (63). Then, mTOR regulates protein synthesis through the phosphorylation and inactivation of a repressor of mRNA translation, 4E-BP1, and through the phosphorylation and activation of S6 kinase (S6K1; ref. 18). In this scenario, deregulation of TSC2 or TSC1 may result in the activation of mTOR (and pAkt<sup>Ser473</sup> accumulation) even in the absence of active pAkt<sup>Thr308</sup>. Indeed, this is the case in tuberous sclerosis, a tumor-prone syndrome characterized by the presence of multiple benign hamartomas resulting from the presence of somatic or inherited mutation in TSC1 or TSC2 (64). In line with this possibility, a recent study documented the presence of polymorphisms or mutations in TSC1 and TSC2 in HNSCC cancer patients (65). In addition, the human papillomavirus oncogenic protein E6 has been shown to interact with TSC2, leading to its degradation (66). On the other hand, the activity of TSC2 is stimulated by a cell energy-

sensing kinase, AMPK, which is activated by AMP when the cellular levels of ATP are reduced (67). Surprisingly, recent studies revealed that AMPK is stimulated by a kinase that is the translational product of the *LKB1* tumor-suppressor gene. *LKB1* inactivation leads to a tumor-prone syndrome, Peutz-Jeghers syndrome, that is characterized by the presence of multiple gastrointestinal hamartomas (67, 68). Expression of *LKB1* can be also reduced by epigenetic events such as promoter hypermethylation, as recently shown in HNSCC tumor cell lines (69). Thus, based on these studies and our present findings, we can speculate that mutations in *TSC2*, *TSC1*, or *LKB1*, all tumor-suppressor genes impinging on mTOR, and/or human papillomavirus infections may cooperate in HNSCC development by promoting the activation of mTOR in absence of active Akt.

It is imperative to understand the nature of the dysregulated molecular mechanisms underlying the development of HNSCC, as it will provide a rational foundation to explore new treatment modalities and to stratify patients that may benefit from novel molecular-targeted therapies. The limited clinical response to the treatment of HNSCC patients with EGFR-interfering therapies suggest that during tumor progression, HNSCC lesions may acquire a number of genetic and epigenetic alterations that result in the persistent activation of growth-promoting pathways, bypassing the requirement of EGFR signaling for cell proliferation. Among these, the activation of Akt, nuclear factor- $\kappa$ B, and signal transducers and activators of transcription 3 seems to play an important role (7, 11). In this regard, the opportunity to analyze simultaneously the level of expression and status of activation of many signaling molecules in hundreds of HNSCC tissues has now revealed that HNSCC may harbor complementary alterations in multiple biochemical routes that converge to activate the Akt-mTOR signaling pathway. This seems to be the case in all HNSCC tissues, regardless of their site of origin, as we did not find any significant difference in the status of Akt-mTOR activation across HNSCC cases from the oral cavity and oropharynx. These findings provide a molecular framework for future exploration of the nature of the regulatory proteins whose alterations are responsible for EGFR-independent activation of mTOR, including aberrant function of phosphatidylinositol 3'-OH kinase, PTEN, TSC1, TSC2, *LKB1*, and/or the activation of other tyrosine kinase receptors. Collectively, our current observations also support the emerging notion that mTOR and its downstream molecules may represent a suitable target for HNSCC treatment, alone or in combination with other standard therapies, as its activation is a common event in most HNSCC lesions, independent of p53 status and EGFR activation levels.

## References

1. Leading sites of new cancer cases and deaths—2007 estimates. Cancer facts and figures 2007. Atlanta: American Cancer Society; 2007.
2. Canto MT, Devesa SS. Oral cavity and pharynx cancer incidence rates in the United States, 1975-1998. *Oral Oncology* 2002;38:610-7.
3. Hashibe M, Brennan P, Benhamou S, et al. Alcohol drinking in never users of tobacco, cigarette smoking in never drinkers, and the risk of head and neck cancer: pooled analysis in the International Head and Neck Cancer Epidemiology Consortium. *J Natl Cancer Inst* 2007;99:777-89.
4. Warnakulasuriya S, Sutherland G, Scully C. Tobacco, oral cancer, and treatment of dependence. *Oral Oncol* 2005;41:244-60.
5. Jemal A, Clegg LX, Ward E, et al. Annual report to the nation on the status of cancer, 1975-2001, with a special feature regarding survival. *Cancer* 2004; 101:3-27.
6. Yu M, Yeh J, Van Waes C. Protein kinase casein kinase 2 mediates inhibitor- $\kappa$ B kinase and aberrant nuclear factor- $\kappa$ B activation by serum factor(s) in head and neck squamous carcinoma cells. *Cancer Res* 2006; 66:6722-31.
7. Leeman RJ, Lui VW, Grandis JR. STAT3 as a therapeutic target in head and neck cancer. *Expert Opin Biol Ther* 2006;6:231-41.
8. Song JI, Grandis JR. STAT signaling in head and neck cancer. *Oncogene* 2000;19:2489-95.
9. Mao L, Hong WK, Papadimitrakopoulou VA. Focus on head and neck cancer. *Cancer Cell* 2004;5: 311-6.
10. Forastiere A, Koch W, Trotti A, et al. Head and neck cancer. *New Engl J Med* 2001;345:1890-900.
11. Amornphimoltham P, Sriuranpong V, Patel V, et al. Persistent activation of the Akt pathway in head and

- neck squamous cell carcinoma: a potential target for UCN-01. *Clin Cancer Res* 2004;10:4029–37.
12. Mandal M, Younes M, Swan EA, et al. The Akt inhibitor KP372-1 inhibits proliferation and induces apoptosis and anoikis in squamous cell carcinoma of the head and neck. *Oral Oncology* 2006;42:430–9.
  13. Tosi L, Rinaldi E, Carinci F, et al. Akt, protein kinase C, mitogen-activated protein kinase phosphorylation status in head and neck squamous cell carcinoma. *Head and Neck* 2005;27:130–7.
  14. Segrelles C, Ruiz S, Perez P, et al. Functional roles of Akt signaling in mouse skin tumorigenesis. *Oncogene* 2002;21:53–64.
  15. Massarelli E, Liu DD, Lee JJ, et al. Akt activation correlates with adverse outcome in tongue cancer. *Cancer* 2005;104:2430–6.
  16. Segrelles C, Moral M, Lara MF, et al. Molecular determinants of Akt-induced keratinocyte transformation. *Oncogene* 2006;25:1174–85.
  17. Easton JB, Houghton PJ. mTOR and cancer therapy. *Oncogene* 2006;25:6436–46.
  18. Hay N, Sonenberg N. Upstream and downstream of mTOR. *Genes and Development* 2004;18:1926–45.
  19. Sorrells DL, Meschonat C, Black D, et al. Pattern of amplification and overexpression of the eukaryotic initiation factor 4E gene in solid tumor. *J Surg Res* 1999;85:37–42.
  20. Nathan CA, Amirghahri N, Rice C, et al. Molecular analysis of surgical margins in head and neck squamous cell carcinoma patients. *Laryngoscope* 2002;112:2129–40.
  21. Amorphimoltham P, Patel V, Sodhi A, et al. Mammalian target of rapamycin, a molecular target in squamous cell carcinomas of the head and neck. *Cancer Res* 2005;65:9953–61.
  22. Hewitt SM. Design, construction, and use of tissue microarrays. *Methods Mol Biol* 2004;264:61–72.
  23. Kononen J, Bubendorf L, Kallioniemi A, et al. Tissue microarrays for high-throughput molecular profiling of tumor specimens. *Nat Med* 1998;4:844–7.
  24. Rossi E, Villanacci V, Bassotti G, et al. Her-2/neu in Barrett esophagus: a comparative study between histology, immunohistochemistry, and fluorescence *in situ* hybridization. *Diagn Mol Pathol* 2006;15:125–30.
  25. Cha YI, Solnica-Krezel L, DuBois RN. Fishing for prostanoids: deciphering the developmental functions of cyclooxygenase-derived prostaglandins. *Dev Biol* 2006;289:263–72.
  26. Lin DT, Subbaramaiah K, Shah JP, et al. Cyclooxygenase-2: a novel molecular target for the prevention and treatment of head and neck cancer. *Head Neck* 2002;24:792–9.
  27. Thomas GR, Nadiminti H, Regalado J. Molecular predictors of clinical outcome in patients with head and neck squamous cell carcinoma. *Int J Exp Pathol* 2005;86:347–63.
  28. Itoh S, Matsui K, Furuta I, et al. Immunohistochemical study on overexpression of cyclooxygenase-2 in squamous cell carcinoma of the oral cavity: its importance as a prognostic predictor. *Oral Oncol* 2003;39:829–35.
  29. Mestre JR, Chan G, Zhang F, et al. Inhibition of cyclooxygenase-2 expression. An approach to preventing head and neck cancer. *Ann N Y Acad Sci* 1999;889:62–71.
  30. Gallo O, Masini E, Bianchi B, et al. Prognostic significance of cyclooxygenase-2 pathway and angiogenesis in head and neck squamous cell carcinoma. *Hum Pathol* 2002;33:708–14.
  31. Peng JP, Chang HC, Hwang CF, et al. Overexpression of cyclooxygenase-2 in nasopharyngeal carcinoma and association with lymph node metastasis. *Oral Oncol* 2005;41:903–8.
  32. El-Naggar AK, Lai S, Luna MA, et al. Sequential p53 mutation analysis of pre-invasive and invasive head and neck squamous carcinoma. *Int J Cancer* 1995;64:196–201.
  33. Taylor D, Koch WM, Zahurak M, et al. Immunohistochemical detection of p53 protein accumulation in head and neck cancer: correlation with p53 gene alterations. *Human Pathol* 1999;30:1221–5.
  34. Vousden KH, Lane DP. p53 in health and disease. *Nat Rev Mol Cell Biol* 2007;8:275–83.
  35. Boyle JO, Hakim J, Koch W, et al. The incidence of p53 mutations increases with progression of head and neck cancer. *Cancer Res* 1993;53:4477–80.
  36. Brennan JA, Boyle JO, Koch WM, et al. Association between cigarette smoking and mutation of the p53 gene in squamous-cell carcinoma of the head and neck. *New Engl J Med* 1995;332:712–7.
  37. Saranath D, Tandle AT, Teni TR, et al. p53 inactivation in chewing tobacco-induced oral cancers and leukoplakias from India. *Oral Oncol* 1999;35:242–50.
  38. Thongsuksai P, Boonyaphiphat P, Sriplung H, et al. p53 mutations in betel-associated oral cancer from Thailand. *Cancer Lett* 2003;201:1–7.
  39. Hitt R, Ciruelos E, Amador ML, et al. Prognostic value of the epidermal growth factor receptor (EGFR) and p53 in advanced head and neck squamous cell carcinoma patients treated with induction chemotherapy. *Eur J Cancer* 2005;41:453–60.
  40. Ford AC, Grandis JR. Targeting epidermal growth factor receptor in head and neck cancer. *Head Neck* 2003;25:67–73.
  41. Kalyankrishna S, Grandis JR. Epidermal growth factor receptor biology in head and neck cancer. *J Clin Oncol* 2006;24:2666–72.
  42. Kong A, Leboucher P, Leek R, et al. Prognostic value of an activation state marker for epidermal growth factor receptor in tissue microarrays of head and neck cancer. *Cancer Res* 2006;66:2834–43.
  43. Honegger A, Dull TJ, Bellot F, et al. Biological activities of EGFR-receptor mutants with individually altered autophosphorylation sites. *EMBO J* 1988;7:3045–52.
  44. Van Schaeybroeck S, Karaiskou-McCauley A, Kelly D, et al. Epidermal growth factor receptor activity determines response of colorectal cancer cells to gefitinib alone and in combination with chemotherapy. *Clin Cancer Res* 2005;11:7480–9.
  45. Cohen RB. Epidermal growth factor receptor as a therapeutic target in colorectal cancer. *Clin Colorectal Cancer* 2003;2:246–51.
  46. Baselga J, Albanell J, Ruiz A, et al. Phase II and tumor pharmacodynamic study of gefitinib in patients with advanced breast cancer. *J Clin Oncol* 2005;23:5323–33.
  47. Herbst RS, Prager D, Hermann R, et al. TRIBUTE: a phase III trial of erlotinib hydrochloride (OSI-774) combined with carboplatin and paclitaxel chemotherapy in advanced non-small-cell lung cancer. *J Clin Oncol* 2005;23:5892–9.
  48. Sriuranpong V, Park JI, Amorphimoltham P, et al. Epidermal growth factor receptor-independent constitutive activation of STAT3 in head and neck squamous cell carcinoma is mediated by the autocrine/paracrine stimulation of the interleukin 6/gp130 cytokine system. *Cancer Res* 2003;63:2948–56.
  49. Stephens L, Anderson K, Stokoe D, et al. Protein kinase B kinases that mediate phosphatidylinositol 3,4,5-trisphosphate-dependent activation of protein kinase B. *Science* 1998;279:710–4.
  50. Hresko RC, Mueckler M. mTOR RICTOR is the Ser473 kinase for Akt/protein kinase B in 3T3–1 adipocytes. *J Biol Chem* 2005;280:40406–16.
  51. Hanada M, Feng J, Hemmings BA. Structure, regulation and function of PKB/AKT—a major therapeutic target. *Biochim Biophys Acta* 2004;1697:3–16.
  52. Luo J, Manning BD, Cantley LC. Targeting the PI3K-Akt pathway in human cancer: rationale and promise. *Cancer Cell* 2003;4:257–62.
  53. Singh B, Stoffel A, Gogineni S, et al. Amplification of the 3q26.3 locus is associated with progression to invasive cancer and is a negative prognostic factor in head and neck squamous cell carcinomas. *Am J Pathol* 2002;161:365–71.
  54. Pedrero JM, Carracedo DG, Pinto CM, et al. Frequent genetic and biochemical alterations of the PI 3-K/AKT/PTEN pathway in head and neck squamous cell carcinoma. *Int J Cancer* 2005;114:242–8.
  55. Woenckhaus J, Steger K, Werner E, et al. Genomic gain of PIK3CA and increased expression of p110 $\alpha$  are associated with progression of dysplasia into invasive squamous cell carcinoma. *J Pathol* 2002;198:335–42.
  56. Kozaki K, Imoto I, Pimkhaokham A, et al. PIK3CA mutation is an oncogenic aberration at advanced stages of oral squamous cell carcinoma. *Cancer Sci* 2006;97:1351–8.
  57. Bader AG, Kang S, Vogt PK. Cancer-specific mutations in PIK3CA are oncogenic *in vivo*. *Proc Natl Acad Sci U S A* 2006;103:1475–9.
  58. Lee JI, Soria JC, Hassan KA, et al. Loss of PTEN expression as a prognostic marker for tongue cancer. *Arch Otolaryngol Head Neck Surg* 2001;127:1441–5.
  59. Dong G, Lee TL, Yeh NT, et al. Metastatic squamous cell carcinoma cells that overexpress c-Met exhibit enhanced angiogenesis factor expression, scattering and metastasis in response to hepatocyte growth factor. *Oncogene* 2004;23:6199–208.
  60. Khan AJ, King BL, Smith BD, et al. Characterization of the HER-2/neu oncogene by immunohistochemical and fluorescence *in situ* hybridization analysis in oral and oropharyngeal squamous cell carcinoma. *Clin Cancer Res* 2002;8:540–8.
  61. Shamji AF, Nghiem P, Schreiber SL. Integration of growth factor and nutrient signaling: implications for cancer biology. *Mol Cell* 2003;12:271–80.
  62. Inoki K, Corradetti MN, Guan KL. Dysregulation of the TSC-mTOR pathway in human disease. *Nat Genet* 2005;37:19–24.
  63. Manning BD, Cantley LC. Rheb fills a GAP between TSC and TOR. *Trends Biochem Sci* 2003;28:573–6.
  64. Crino PB, Nathanson KL, Henske EP. The tuberous sclerosis complex. *N Engl J Med* 2006;355:1345–56.
  65. Hebert C, Norris K, Parashar P, et al. Hypoxia-inducible factor-1 $\alpha$  polymorphisms and TSC1/2 mutations are complementary in head and neck cancers. *Mol Cancer* 2006;5:3.
  66. Lu Z, Hu X, Li Y, et al. Human papillomavirus 16 E6 oncoprotein interferes with insulin signaling pathway by binding to tuberlin. *J Biol Chem* 2004;279:35664–70.
  67. Martin DE, Hall MN. The expanding TOR signaling network. *Curr Opin Cell Biol* 2005;17:158–66.
  68. McGarrity TJ, Amos C. Peutz-Jeghers syndrome: clinicopathology and molecular alterations. *Cell Mol Life Sci* 2006;63:2135–44.
  69. Qiu W, Schonleben F, Thaker HM, et al. A novel mutation of STK11/LKB1 gene leads to the loss of cell growth inhibition in head and neck squamous cell carcinoma. *Oncogene* 2006;25:2937–42.